Electronic Supplementary Material (ESI) for Physical Chemistry Chemical Physics.

Supporting Information for: Structural effects in nanotribology of nanoscale films of ionic liquids confined between metallic surfaces

Silvia Di Lecce,[†] Alexei A. Kornyshev,[†] Michael Urbakh,[‡] and Fernando Bresme*,[†]

†*Department of Chemistry, Molecular Sciences Research Hub, Imperial College London, W12 0BZ London, United Kingdom*

‡*School of Chemistry and The Sackler Center for Computational Molecular and Materials Science, Tel Aviv University, 69978, Tel Aviv, Israel*

E-mail: f.bresme@imperial.ac.uk

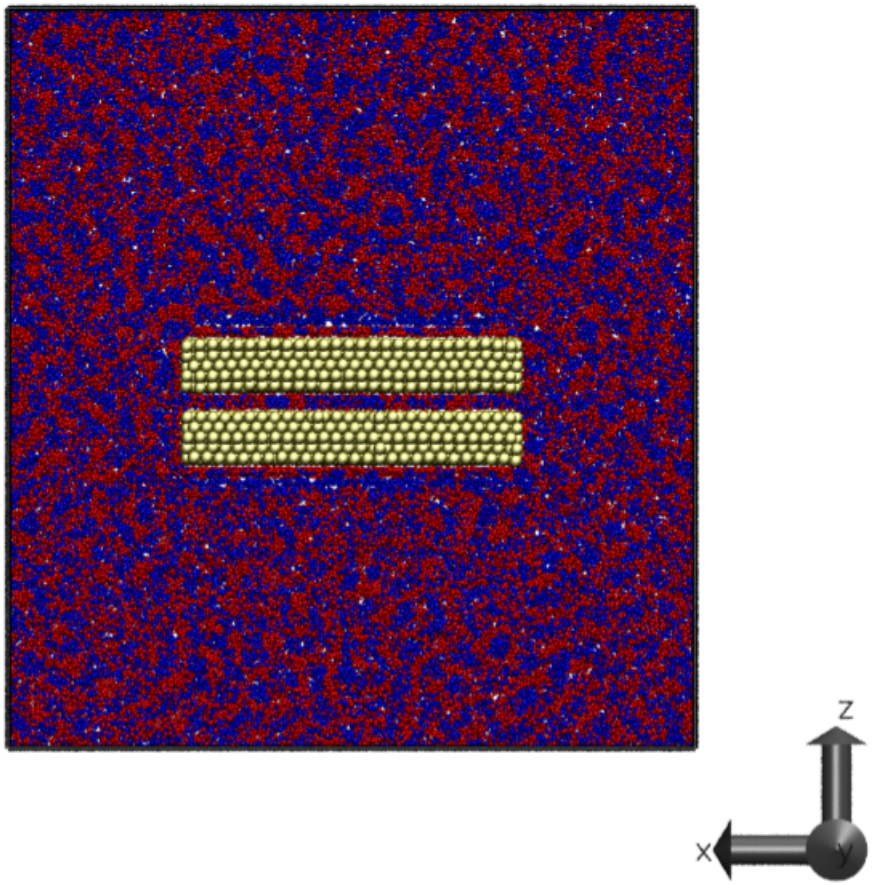

Figure S1: Snapshot of the simulation set–up employed in this work. The gold slabs, represented with yellow spheres are immersed in the ionic liquid $[C_2MIM]^+$ $[NTf_2]^-$. For enhanced visibility, all the atoms in the cations are represented as red spheres, and the atoms in the anions as blue spheres. The snapshot was generated using the VMD software.[1]

Friction coefficient The dependence of the friction force, F_f, with normal load, F_L, shown in Figure 2 of the main text, has been be fitted using a modified Amontons' law, $F_f = a + \mu F_L$, where the slope μ is the friction coefficient and a the friction force at zero load, which is > 0 for adhesive forces. We show in Figure S2 the corresponding friction coefficients. Further, we compare our results with data from Ref. 2 for the friction force of $[C_2MIM]^+$ $[NTf_2]^-$ confined between negatively and positively charged surfaces with a lattice parameter of 0.36 nm.

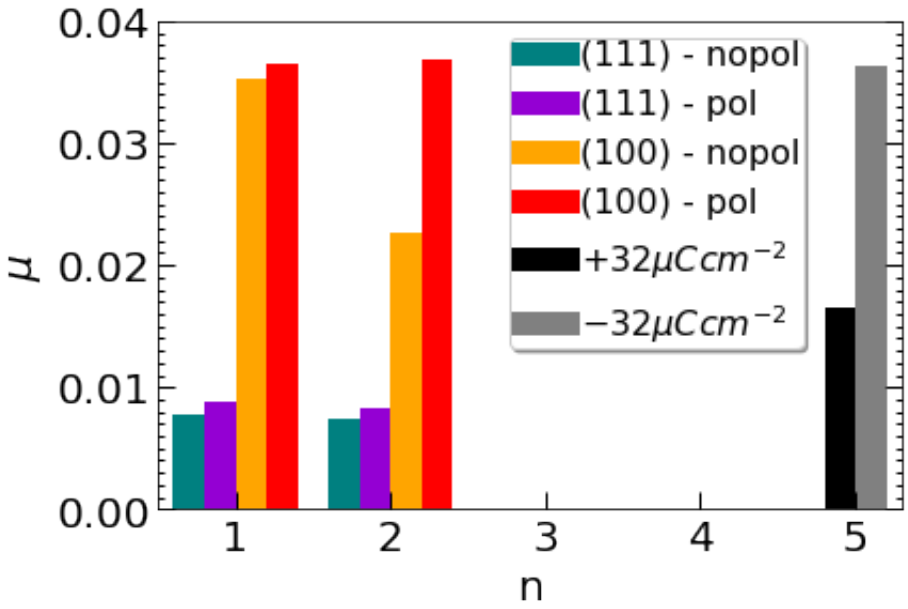

Figure S2: Friction coefficient μ for different (100) and (111) confining surfaces, polarizable and nopolarizable substrates, and confined layers n. The data for positively and negatively charged surfaces are taken from Ref. 2, where $[C_2MIM]^+$ $[NTf_2]^-$ is confined between (111) charged plates with a surface charge density of ± 32 μC cm^{-2}.

Structure Factor calculations The structure factor, $S_m(k_x, k_y)$, was obtained using the following equation:

$$S_m(\boldsymbol{k}_\xi) = \frac{1}{N_m} \left| \sum_j^{N_m} \exp\left(-i\boldsymbol{k}_\xi \cdot \boldsymbol{r}_j^{(m)}\right) \right|^2 , \tag{1}$$

where $\boldsymbol{k}_\xi = -n_\xi \pi / l_\xi \cdots n_\xi \pi / l_\xi$, are the wave vectors in the $\xi = x, y$, $|n_\xi| = 40$, $l_\xi = 3.5$ nm is the length of the squared confining area used for the calculation, and $\boldsymbol{r}_j^{(m)} = (x_j, y_j)$ are the coordinates of the N_m ions in the m-th layer. The calculations using $\boldsymbol{r}_j^{(m)} = (x_j, y_j)$ were performed with the coordinates of the center of mass of cations and anions. As a reference, we show in Figure S3 the structure factor of the gold layers in direct contact with the RTIL. That structure factor is consistent with a honeycomb lattice for Au{111} and with a square lattice for Au{100} (see Figure S3).

Structural properties of the gold surfaces The normalised 2D density profile of the gold latyer in contact with the confined ionice liquid is shown in Fig. S3 (a, b) for Au(111)

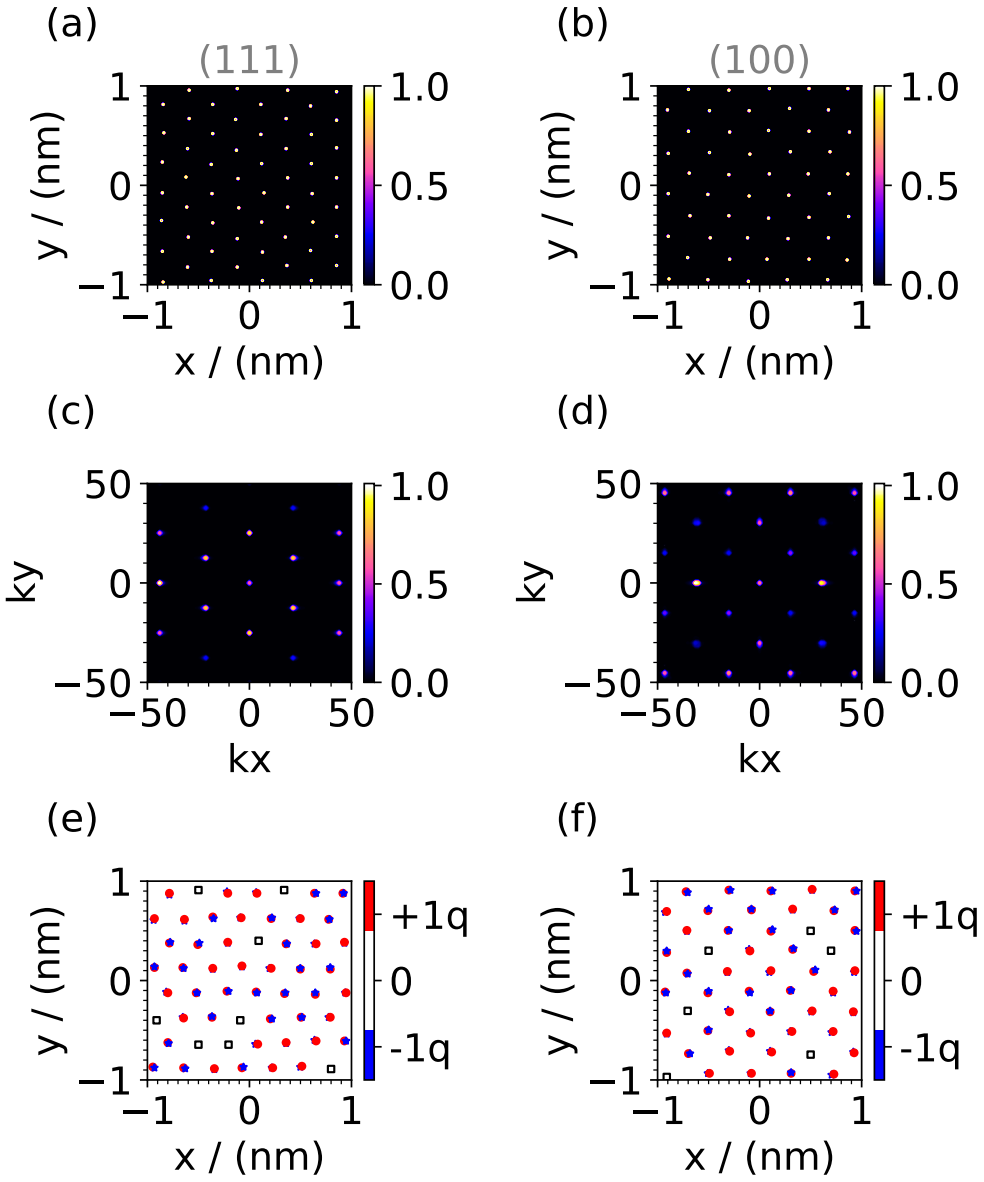

Figure S3: Structural properties of the gold layers in direct contact with the confined ionic liquid, for the two different substrates Au(111) (a, c, e) and Au(100) (b, d, f). Normalised number density (a, b) in the xy direction, structure factor (c, d) and charge distribution on the plane (e, f).

and Au(100) lattice, respectively. We used eq. (1) to calculate the structure factor $S_m(\boldsymbol{k}_\xi)$ of the contact layers (see Fig. S3 (c, d)). The structure factor was normalized by the value of the highest maximum. The charge distribution shown in Fig. S3 (e, f) was computed considering the position of the core and shell particles in the (x, y) plane. When the shell particle is at the same position as the core atom, there is no polarization. This situation is indicated with white squares. Positive charges are indicated with red symbols and negative charges with blue symbols.

The 3D projection of the normalised number density on the xy plane is shown in Figure S4 for Au(111) and Au(100), both polarizable and non-polarizable models. For the polarizable model, we considered both the shell particle and the core particle in the gold lattice.

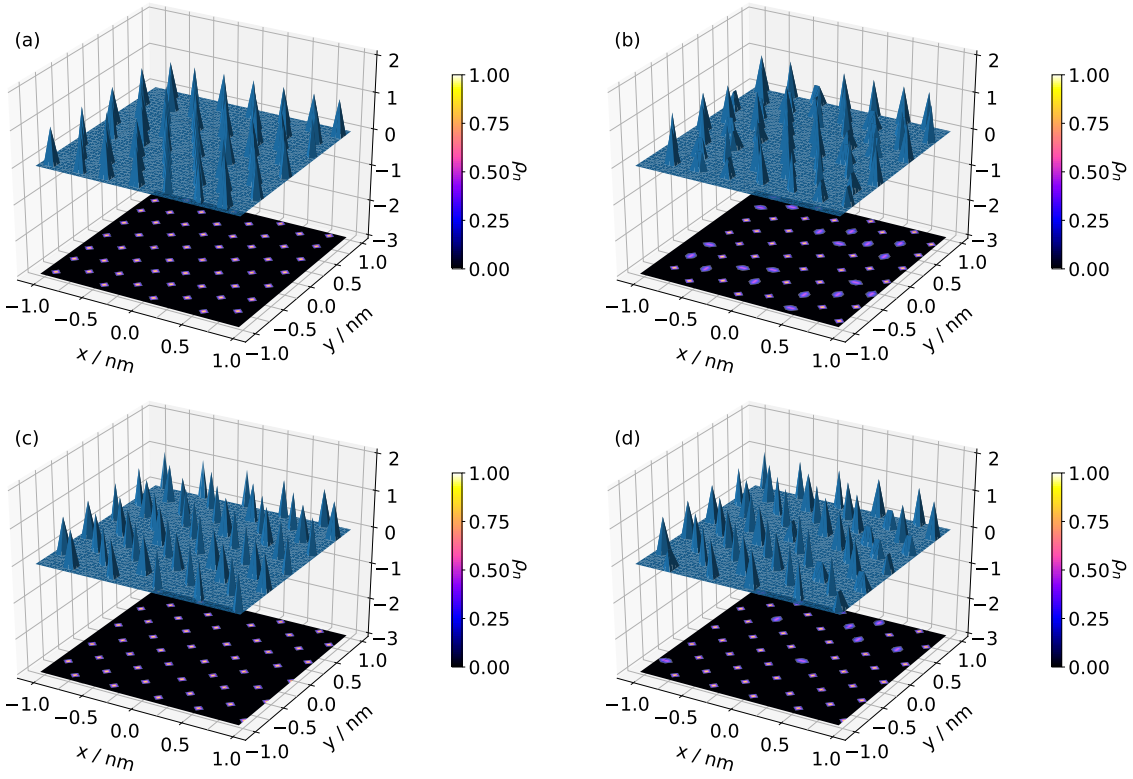

Figure S4: 3D and 2D normalised number densities on the xy plane of the gold atoms in contact with the confined ionic liquid. (a) Au(111) non polarizable (b) Au(111) non polarizable, (c) Au(100) non polarizable and (d) Au(100) polarizable.

Dependence of the friction force with the size of the shell particle in the polarizable We performed additional simulations changing the size of the shell particle in the polarizable model of gold, to investigate the impact of the shell particle on the friction force. The results are shown in Figure S5. The Lennard Jones and Coulombic parameters we changed are the σ_e of the shell particle and the charge q of the shell (e) and core (c) particles. We reduced the σ_e to 0.131228 nm and 0.0874853 nm keeping the charges to the initial values, $q_c = +1$ and $q_e = -1$ (green circle and yellow cross, respectively). We also performed simulations at $q_c = q_e = 0$ and using the original parameters for the size of the shell particle (see red stars).

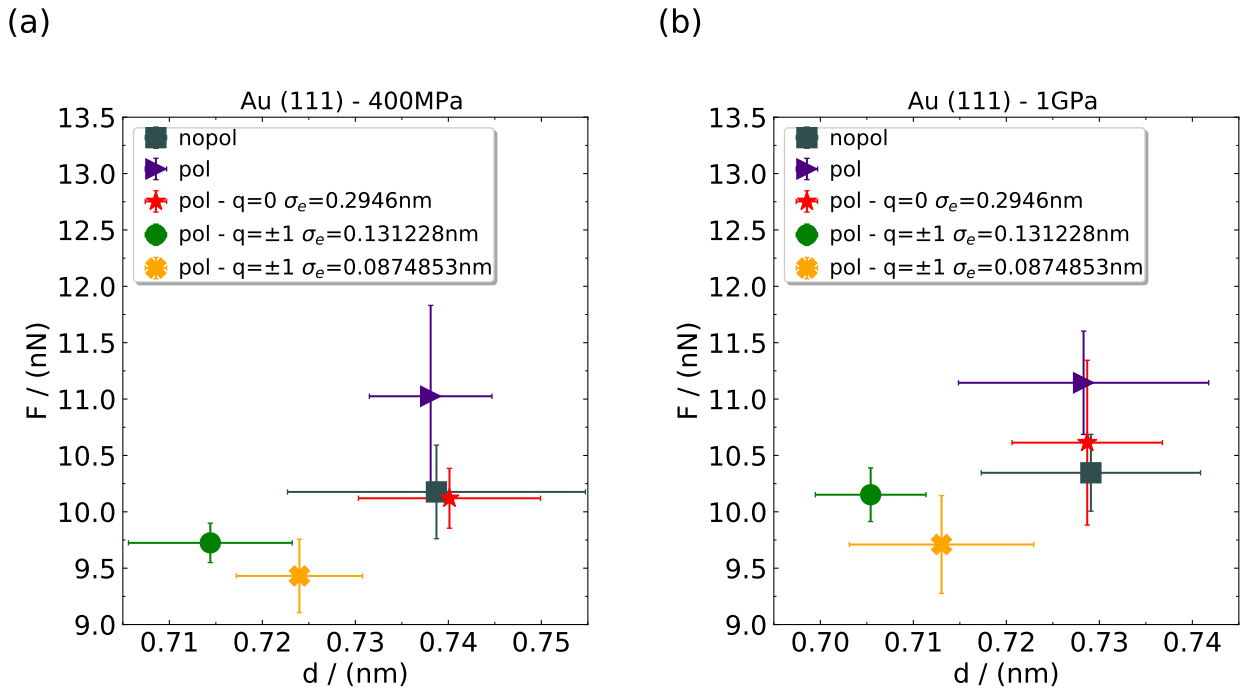

Figure S5: Friction force vs slab separation for $[C_2MIM]^+$ $[NTf_2]^-$ confined between the (111) gold slabs under a load of 0.4GPa (a) and 1GPa (b). Polarizable and non polazible models are indicated using "pol" and "nopol", respectively. For the "pol" model, q is the original charge of the forcefield (+1e, core, and -1, shell). σ_e is the Lennard Jones diameter of the shell particle .

Radial distribution function The radial distribution functions (RDFs) of $[C_2MIM]^+$ $[NTf_2]^-$, were computed using the center of mass of the cation and the anion (see Figure S6). RDFs were obtained using equilibrium NPT simulations of bulk liquids at 350K and 1bar. The simulations consisted of 100 pairs of $[C_2MIM]^+$ $[NTf_2]^-$ and the analysis was performed using trajectories spanning 20 ns.

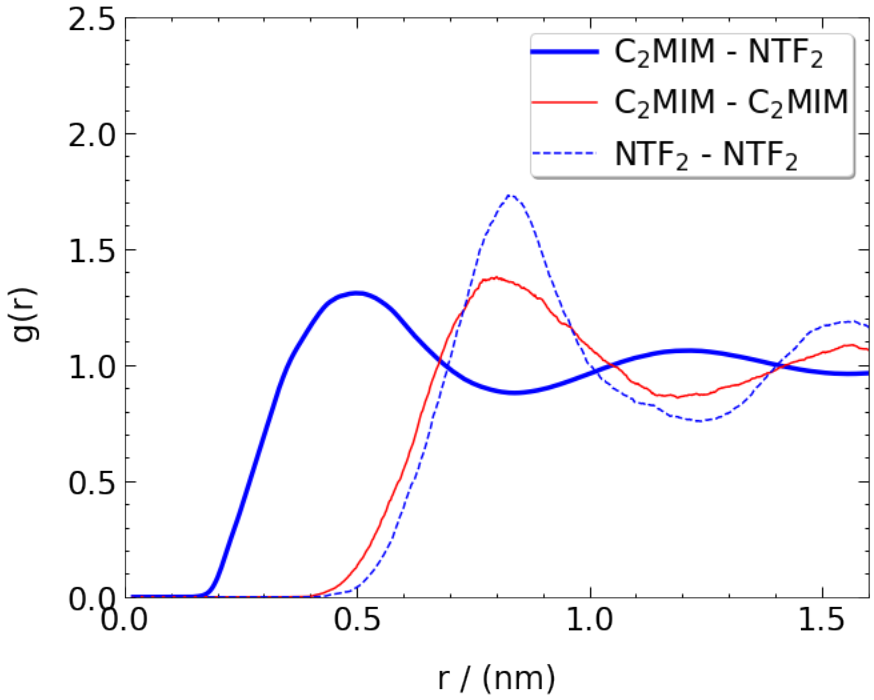

Figure S6: Radial distribution functions of $[C_2MIM]^+$ $[NTf_2]^-$, between the center of mass of the cation and of the anion.

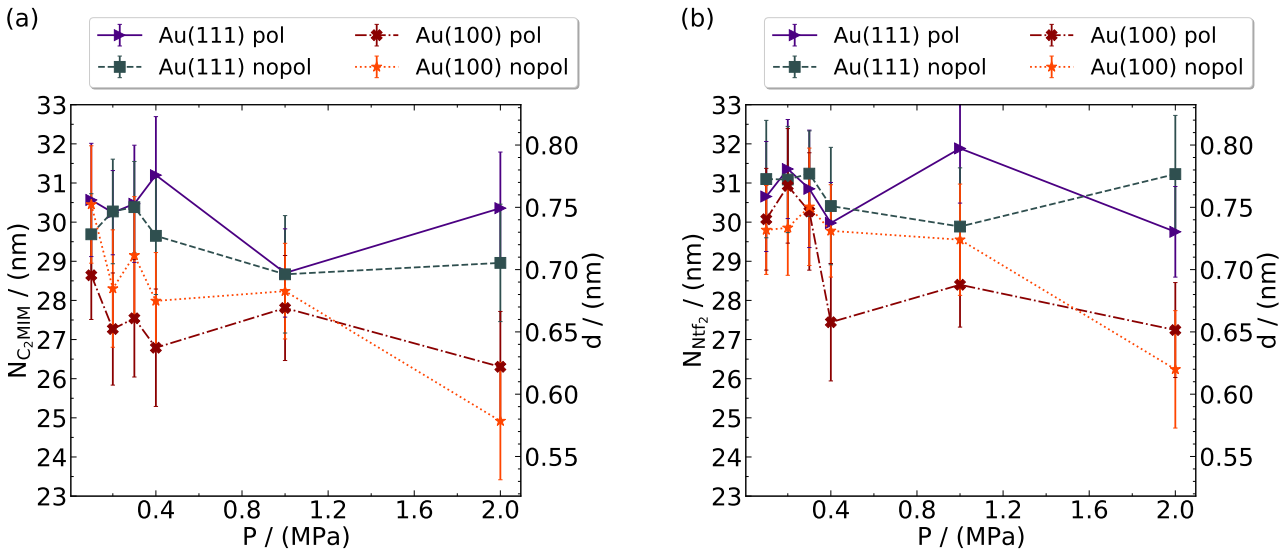

Figure S7: Number of cations (a) and anions (b) in the confined region (left axis) and slab–slab distance d (right axis) as a function of the normal load.

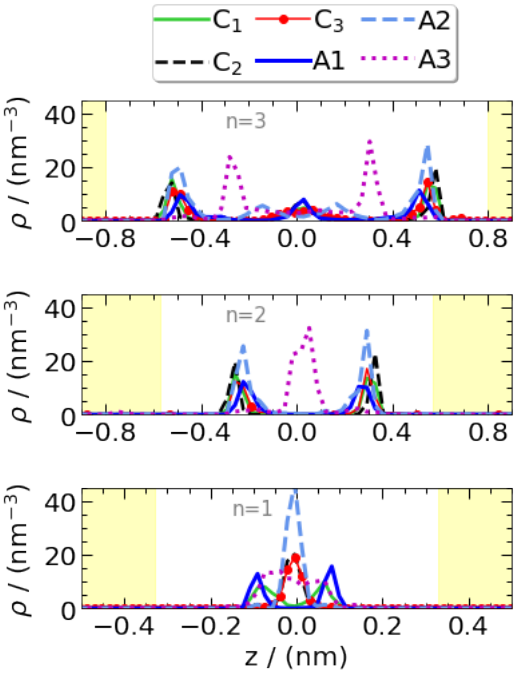

Figure S8: Number density profiles in the direction normal to the gold surfaces (z), for $n = 3$, 0.1 GPa (top), $n = 2$, 0.3 GPa (center) and $n = 1$, 0.4 GPa (bottom). All the data correspond to the Au(111)-nopol surfaces. The coloured area indicates the location of the gold plates.

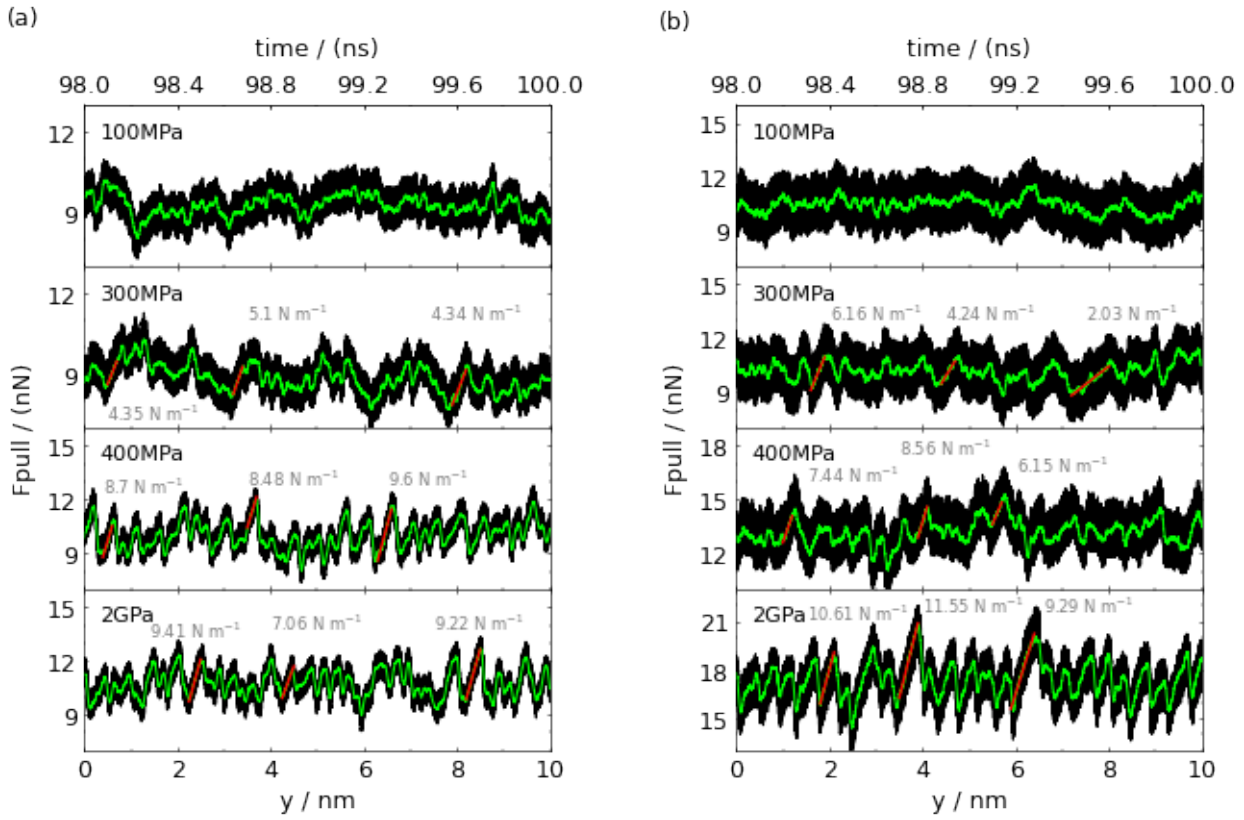

Figure S9: Friction force-displacement and friction force-time curves for $[C_2MIM]^+$ $[NTf_2]^-$ confined between Au(111) (a) and Au(100) (b) non polarizable model and different external load, as specified for each panel. The red lines are linear fittings to the simulated data. The corresponding force constants are given by the numbers next to each curve.

Potential energy curves: The potential energy of the ions sliding on the surfaces were computed as follows. We used an equilibrated configuration of the non-polarizable systems under shear and selected randomly eight ion pairs in the confined region (see Figure S10). We calculated the potential energy of the ions as a function of displacement from the equilibrium position driving the ions along the y direction (the direction of pulling in the non-equilibrium simulations). The displacement (21 points in a 1 nm interval) was applied to the ions' centre of mass, keeping the molecules rigid during this process. The atoms on the surface were not allowed to move either. The potential energy includes the dispersion interactions only as the test surfaces are non-polarizable.

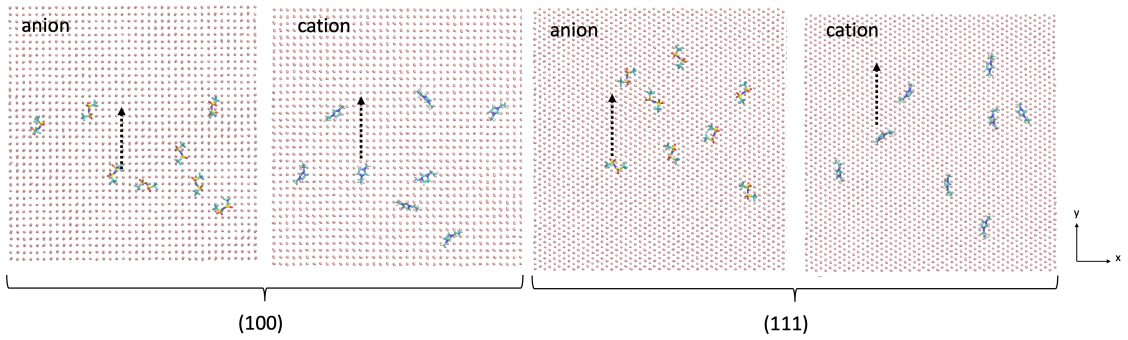

Figure S10: The snapshots show the cations and anions used to compute the potential energies of the ions sliding on (111) and (100) surfaces. The arrow indicates the direction of the displacement of the ions along the y coordinate. Only the Au bottom surface is shown (red dots in the background behind the ions). The Au-top surface has been removed to allow the visualization of the ions in the confined region.

Figure S11 shows the sliding potential energy curves for each ion with the surface. The potential energy represented in the figure corresponds to the ion's interaction with one of the surfaces. The interaction with the other surface shows similar behaviour.

Analysis of imidazolium orientation: We performed additional equilibrium simulations of confined monolayers RTIL to address the impact of non-equilibrium conditions and confinement on the orientation of the imidazolium rings discussed in the main paper (Tables 1, 2 and S1, S2).

We constructed monolayers of RTIL (10 ion pairs) confined between (111) surfaces (see Figure S13). We extracted the ion and gold coordinates from a previous non-equilibrium

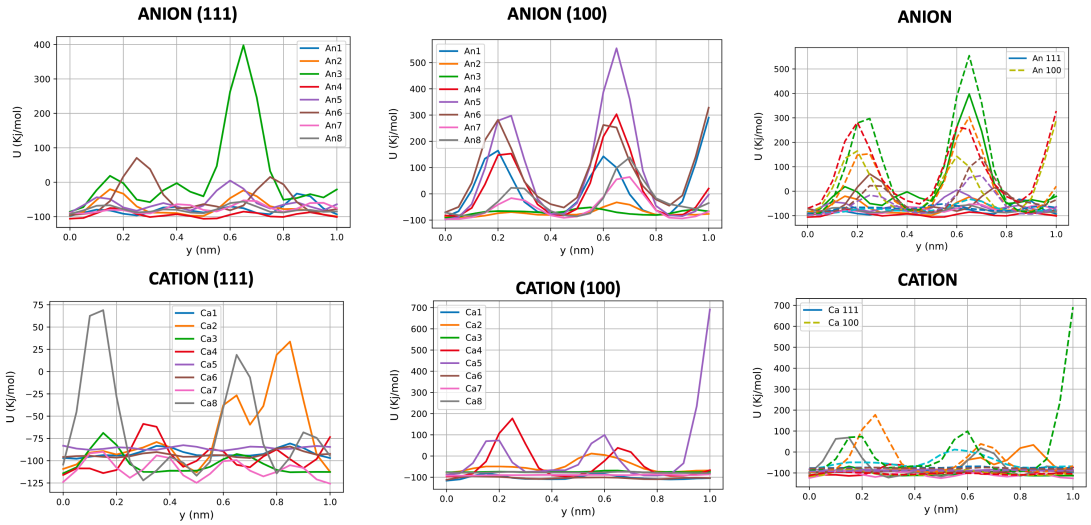

Figure S11: Interaction of the ions with one of the surfaces for (111)-left, (100)-middle. The two panels on the right represent the (111) and (100) results together, to highlight the differences in activation energy between these two surfaces. Note the different y-scale for (111) and (100) data in the left and right panels, respectively.

simulation performed at 400 MPa. We generated two configurations: unconfined, by removing one of the gold slabs (see Figure S13-bottom) and confined, with both gold slabs present (see Figure S13-top). We used the same starting configuration for the monolayers, with the rings in a tilted orientation. The monolayers were simulated for 60 ns. The snapshots for times 0, 1, 4 and 60 ps are shown in Figure S13, and top views of the monolayer structure on gold are also shown for times 0 and 60 ps.

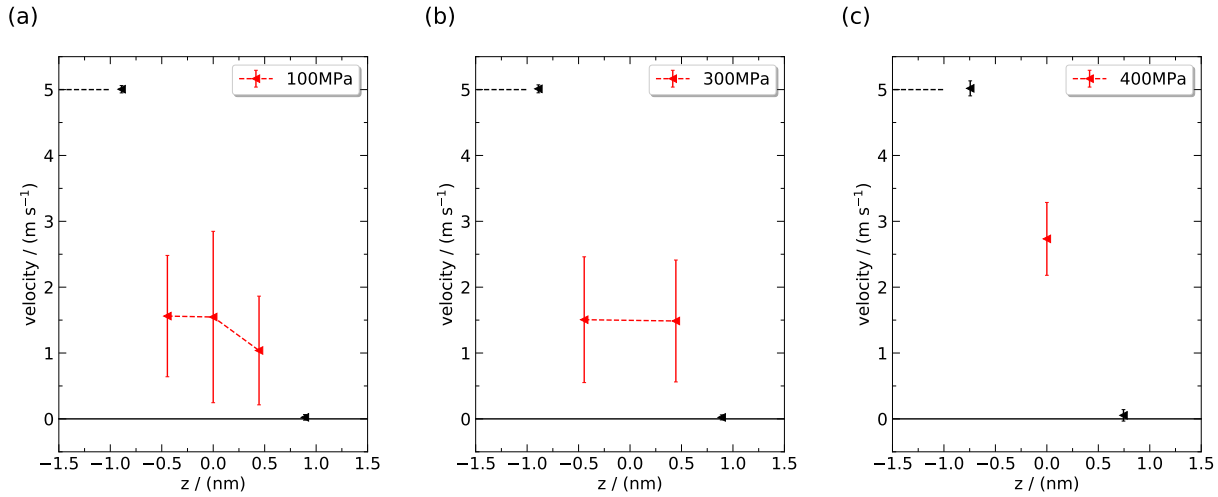

Figure S12: Velocity profiles for the the ionic layers in the confined region and different pressures/film thicknesses, 100 MPa, n = 3, (a), 300 MPa, n = 2 (b) and 400 MPa, n = 1 (c) for Au(111) non-polarizable model. The red points represent the velocities of the ions layers, and the black points dashed line the velocity of the confining walls. The velocity profiles were obtained by analysing the displacement of the ions; the calculated error in the calculation is shown by the error bars.

References

(1) Humphrey, W.; Dalke, A.; Schulten, K. VMD – Visual Molecular Dynamics. *J. Mol. Graph* **1996**, *14*, 33–38.

(2) Di Lecce, S.; Kornyshev, A. A.; Urbakh, M.; Bresme, F. Lateral Ordering in Nanoscale Ionic Liquid Films between Charged Surfaces Enhances Lubricity. *ACS Nano* **2020**, *14*, 13256–13267.

Table S1: Pressure-induced modification of the structure of the $[C_2MIM]^+$ $[NTf_2]^-$ nanofilm confined between gold slabs Au (111) - nopol. The green lines highlight regions with local order.

	Snapshots (side and top views) showing the position of the anions and the cations confined between the Au(111) nopol plates	2D-structure factor $S_m(k_x, k_y)$ for the first layer of RTIL normalised by the maximum value $S_{m,\mathrm{MAX}}$.	Normalised probability distribution function (PDF) of the orientation of the cations (left) and anions (right) adsorbed at the surface. θ represents the angle between the vector indicated in the snapshots and the unit vector parallel to the surface.
100MPa, n=3	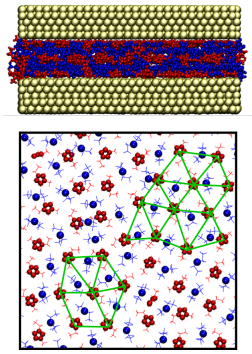	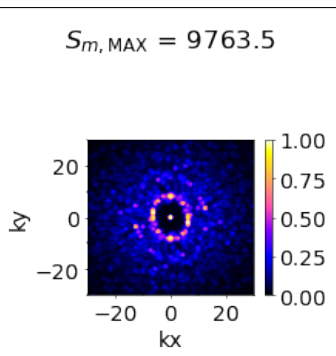	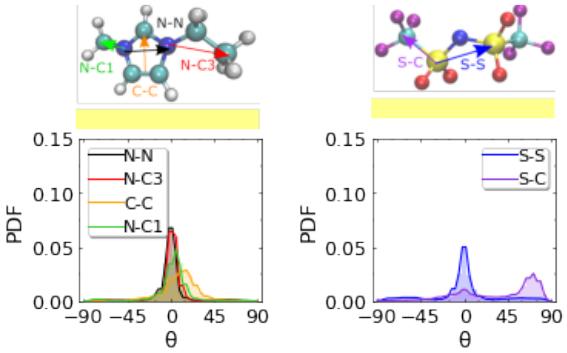
300MPa, n=2	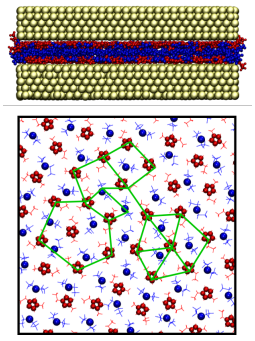	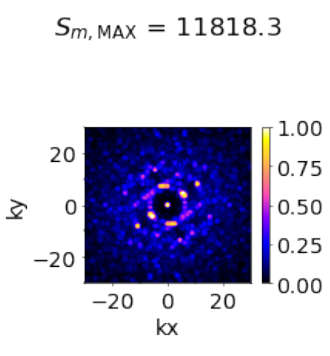	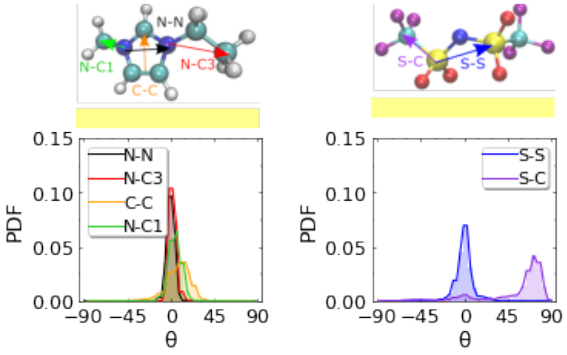
400MPa, n=1	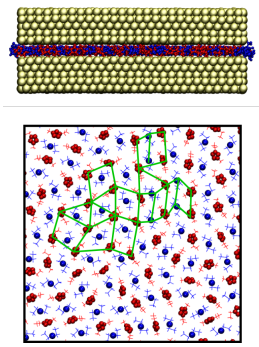	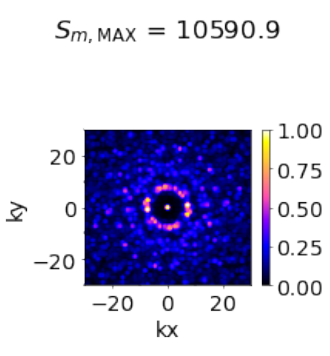	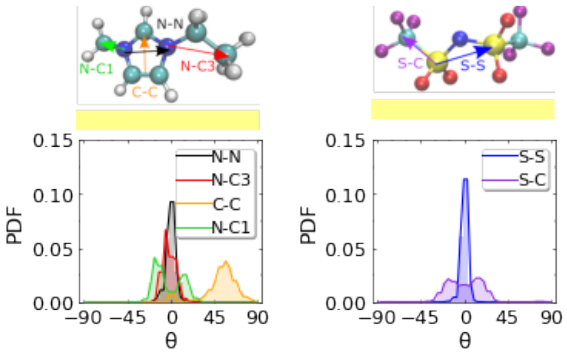
2GPa, n=1	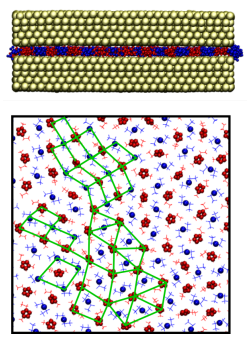	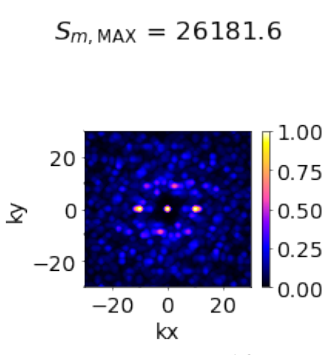	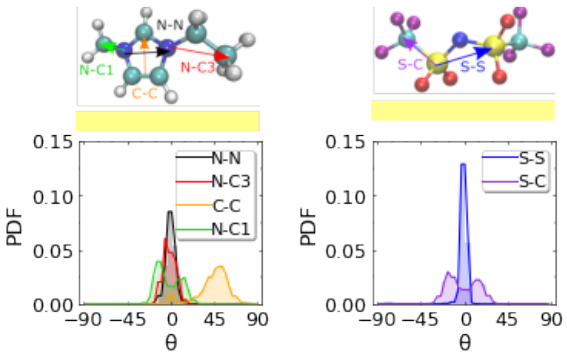

Table S2: Pressure-induced modification of the structure of the $[C_2MIM]^+$ $[NTf_2]^-$ nanofilm confined between gold slabs Au {100} - nopol. The gree lines joining cations and aniones in the left panels highlight the formation of in-plane ordered structures.The green lines highlight regions with local order.

	Snapshots (side and top views) showing the position of the anions and the cations confined between the Au(100) nopol plates	2D-structure factor $S_m(k_x, k_y)$ for the first layer of RTIL normalised by the maximum value $S_{m,\mathrm{MAX}}$.	Normalised probability distribution function (PDF) of the orientation of the cations (left) and anions (right) adsorbed at the surface. θ represents the angle between the vector indicated in the snapshots and the unit vector parallel to the surface.
100MPa, n=3	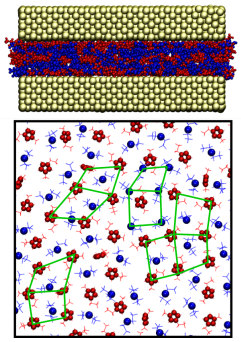	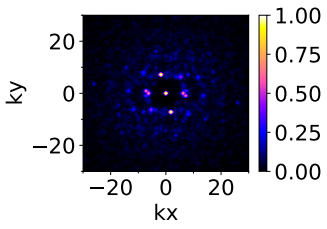	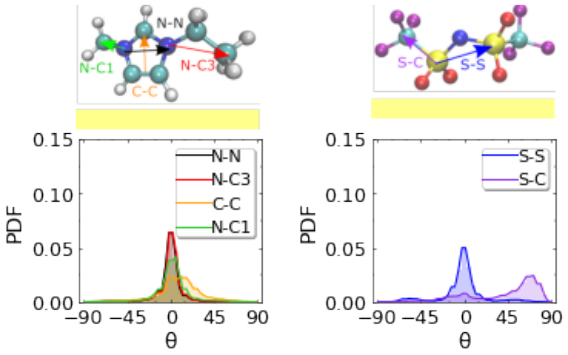
300MPa, n=2	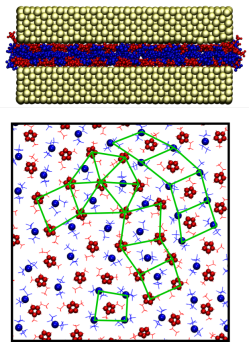	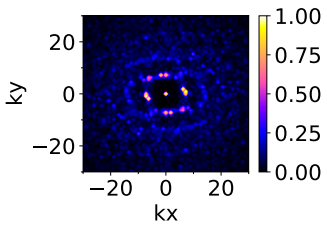	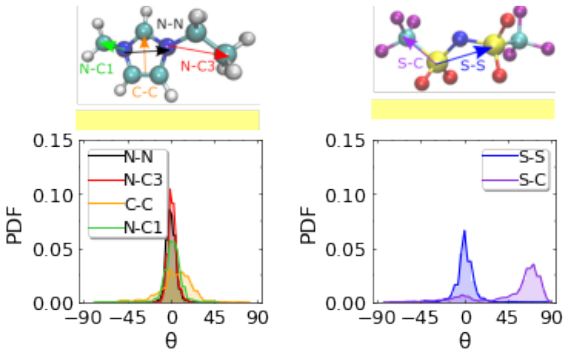
400MPa, n=1	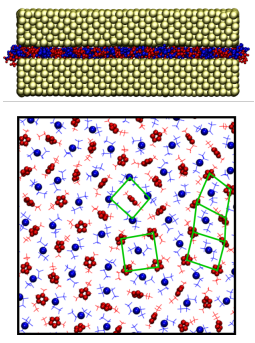	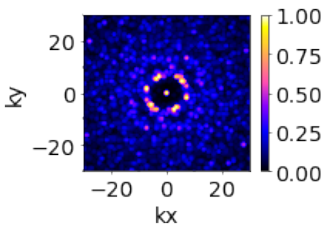	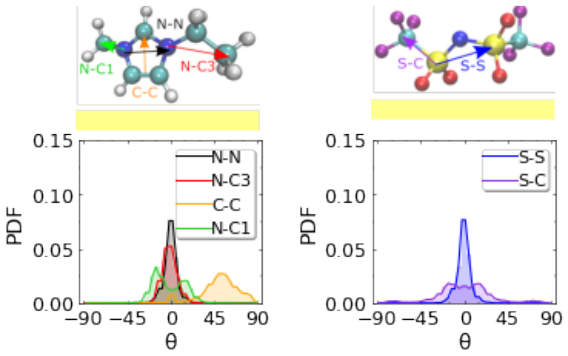
2GPa, n=1	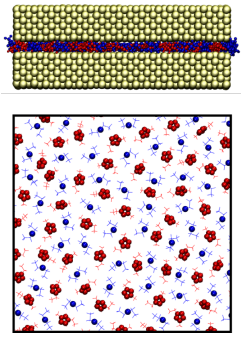	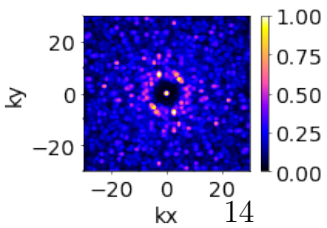	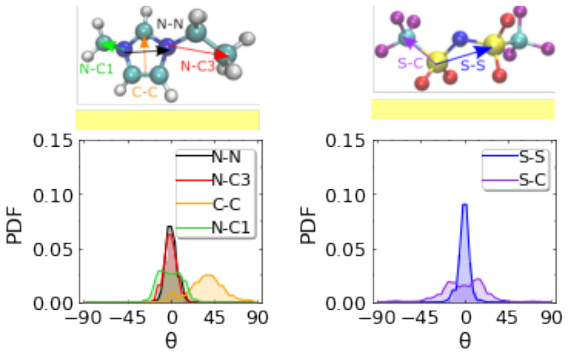

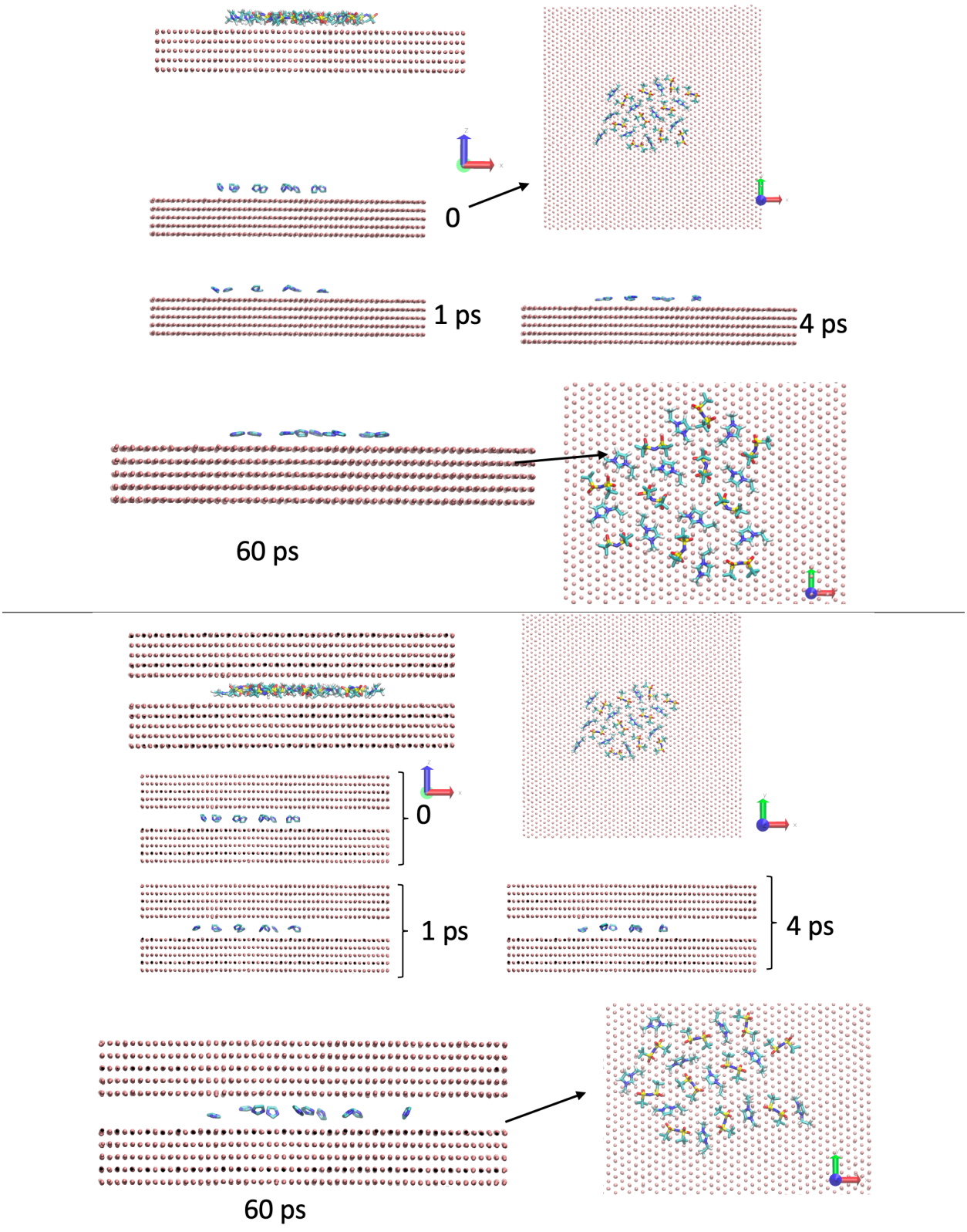

Figure S13: Monolayers consisting of 10 ions pairs adsorbed on the (111) gold surface (non-polarizable). Unconfined (bottom) and confined conditions, corresponding to a load of 400 MPa (top). The starting ion configuration for confined and unconfined simulations is the same. Top views of the monolayer are shown at times 0 ps and 60 ps. The imidazolium ring of the cation lies flat on the surface for the unconfined case (bottom) but features an apparent tilt for the confined case (top).